

Nuclear level-density parameters of nuclei in the $Z \sim 70$ and $A \sim 180$ mid-shell regions

Y. K. Gupta,* D. C. Biswas, Bency John, B. K. Nayak, A. Saxena, and R. K. Choudhury

Nuclear Physics Division, Bhabha Atomic Research Centre, Trombay, 400085 Mumbai, India

(Received 2 April 2009; revised manuscript received 15 July 2009; published 25 November 2009)

α -particle evaporation energy spectra have been measured as a function of γ -ray fold for various target-projectile systems leading to residual nuclei in the range of $Z \sim 70$ and $A \sim 180$ with excitation energy of 30–40 MeV. The inverse level-density parameter K was determined for various nuclei by comparing the high-energy part of the α -particle evaporation spectra with PACE2 predictions. It is observed that the inverse level-density parameter remains constant for all systems studied in this work within statistical errors in the angular momentum range of 15–30 \hbar . The fold-gated α -particle energy spectra in these systems are well reproduced by the PACE2 code with a level-density parameter value of $A/(8.2 \pm 1.1)$ MeV⁻¹.

DOI: [10.1103/PhysRevC.80.054611](https://doi.org/10.1103/PhysRevC.80.054611)

PACS number(s): 21.10.Ma, 25.70.Gh, 24.60.Dr, 27.70.+q

I. INTRODUCTION

The study of nuclear level-density (NLD) parameter a and its dependence on mass and angular momentum is important because it plays a major role in the statistical model in the determination of the phase space available for excited nuclei governing their decay probability. Experimental information on the nuclear level-density parameter comes from two major sources: thermal neutron capture resonance at low excitation energies and angular momenta [1], and particle evaporation spectra in heavy-ion fusion reactions at high excitation energies and angular momenta [2]. Neutron capture resonance studies are confined to a narrow band of nuclei around the β -stability line with low spins and excitation energy equal to the neutron binding energy [3,4]. The major source of knowledge about level densities at higher excitation energies and spins arises from particle-evaporation spectra in heavy-ion fusion reactions analyzed in the framework of the statistical model [5–7]. The level-density parameters obtained in evaporation studies are quantities averaged over a range of excitation energies and angular momenta. Particle evaporation studies with angular momentum selection, done in later years, were devoted to investigating either the deformation effects in nuclei [8] or to understanding the angular momentum window in incomplete fusion reactions [9,10]. Experimental information on angular momentum dependence of the level-density parameter is severely limited and, as a result, the value of a at high angular momentum is essentially unknown for a great majority of nuclei. The study of the level density is also important for heavy nuclei at elevated angular momenta because this is directly related to the issue of stability of heavy nuclei during their synthesis.

In one of our earlier works [11], we investigated the inverse level-density parameter K ($K = A/a$) as a function of angular momentum by measuring γ -ray fold-gated α -particle evaporation spectra in heavy-ion fusion reactions. The residual nuclei after α -particle emission were in the mass region $A_R \sim 120$, charge $Z_R \sim 50$, and with excitation energy in the range of 30–40 MeV. It was observed that for nuclei below

and above $Z_R = 50$ shell closure, the inverse level-density parameter K has a strong dependence on angular momentum in the range of 15–30 \hbar . In this work we have extended our investigation of the level-density parameter as a function of angular momentum to midshell nuclei in the same angular momentum range of 15–30 \hbar . The reactions were selected to populate residual nuclei in the region ($A_R \sim 180$, $Z_R \sim 70$) and the bombarding energies were chosen such that all of the compound nuclei are formed with ~ 57 -MeV excitation energy.

For this study we focus on the high-energy part of the α -particle evaporation energy spectra. By tagging the α -particle energy spectra with γ -ray fold signal, the sensitivity of the level-density parameter with angular momentum was investigated. The K values at the angular momentum range of 15–30 \hbar were extracted by fitting the experimental fold-gated α -particle energy spectra with simulated spectra using the PACE2 code [12].

This article has been organized in the following way. The experimental setup is described in Sec. II, and the data analysis in Sec. III. The results and discussion are presented in Sec. IV. Finally, the summary is presented in Sec. V.

II. EXPERIMENTAL DETAILS

The experiment was performed using the heavy-ion beams of ¹¹B, ¹²C, and ¹⁶O from the BARC-TIFR 14-MV Pelletron accelerator facility at Mumbai. A compact scattering chamber and a γ -ray multiplicity setup consisting of 14 bismuth germinate (BGO) detectors were used for the measurements. Self-supporting metallic foils of ¹⁶⁴Dy (1.1 mg/cm²) and ¹⁸¹Ta (1.5 mg/cm²) were used in the experiment. The α -particles emitted in the reactions were detected by two silicon surface barrier ΔE - E (28 μ m–2 mm) detector telescopes mounted in a reaction plane at $\theta_{\text{lab}} = 125^\circ$ and 153° with respect to beam direction. The telescopes were of equal solid angles of 5.94 mSr. Another surface-barrier detector having a solid angle of 0.20 mSr was mounted at $\theta_{\text{lab}} = 16^\circ$ to measure Rutherford scattering events for normalization and cross-section calculation. The telescopes were energy calibrated in the same way as in the previous work [11]. The various experimental parameters of the reactions studied

* ykgupta@barc.gov.in

TABLE I. The experimental parameters of reactions studied in this work.

Index	Reaction	Z_R	A_R	α	E_{lab} (MeV)	$E_{\text{ex}}^{\text{CN}}$ (MeV)	l_{gr} (\hbar)
a	$^{11}\text{B} + ^{164}\text{Dy}$	69	171	0.874	65	58.4	32
b	$^{12}\text{C} + ^{164}\text{Dy}$	70	172	0.863	74	57.1	33
c	$^{16}\text{O} + ^{164}\text{Dy}$	72	176	0.822	86	56.5	32
d	$^{12}\text{C} + ^{181}\text{Ta}$	77	189	0.875	77	57.0	33

in this work, such as charge Z_R and mass number A_R of residual nuclei after α -particle evaporation, entrance-channel mass-asymmetry parameter α [$\alpha = (A_T - A_P)/(A_T + A_P)$], bombarding energy E_{lab} , compound nucleus excitation energy $E_{\text{ex}}^{\text{CN}}$, and grazing angular momentum value l_{gr} are listed in Table I. The energy threshold of BGO detectors was adjusted to be 100 keV γ -ray energy. The total efficiency of 14 BGO detectors used in this experiment is about 55% at 662 keV. The fold-gated α -particle energy spectra were projected out from the list-mode data after putting a suitable two-dimensional (2D) gate on the α -particle band and on the γ -ray multiplicity fold number. Fold number is defined as the number of BGO detectors firing simultaneously in an event.

The α -particles originating from the reactions with impurity elements such as carbon and oxygen appear in the energy spectra at center-of-mass energies around 4–8 MeV, which is much lower than the 15–25 MeV for the α particles of our interest. This low-energy component has been treated as a background in this analysis. It was observed that this background falls off exponentially as a function of α -particle energy. The grazing angular momentum populated in the fusion reactions with light impurity elements is much less than that of targets. Therefore, this background decreases rapidly as one moves from low to high γ -ray fold events. The α -particle multiplicity, ν_α , is much less (~ 0.01) in this mass region in comparison to the lower mass region $A \sim 120$ previously studied [11], where ν_α is ~ 0.2 . Therefore, the background dominates for low γ -ray folds (up to fold 3) in this mass region. Thus, the analysis has been carried out only for fold 4 and above events, where the background contribution is seen to be negligible. The laboratory α -particle energy spectra were transformed to the center-of-mass system using the standard Jacobian [13]. The center-of-mass energy spectra measured at both the angles overlapped very well for each γ -ray fold as shown in Fig. 1 for two systems, indicating that the spectra originated from the evaporation process. The average α -particle energy spectra obtained at two angles were compared with the PACE2 calculations to derive the level-density parameter.

III. DATA ANALYSIS

The theoretical α -particle energy spectra, as a function of γ -ray fold, were generated using the events file of the statistical model code PACE2 by taking into account the efficiency of the BGO detector setup and the angular momentum removed by γ -rays as discussed in Ref. [11]. The form of the level density

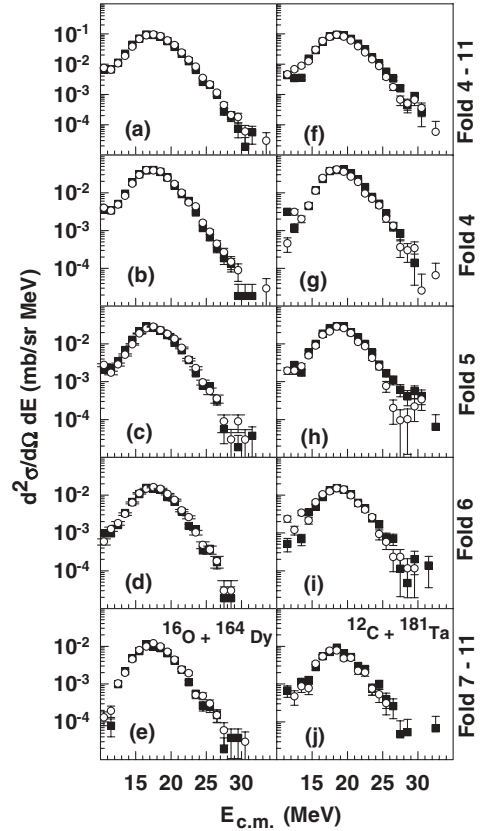


FIG. 1. Center-of-mass α -particle energy spectra measured at $\theta_{\text{lab}} = 125^\circ$ (solid squares) and $\theta_{\text{lab}} = 153^\circ$ (open circles) for various folds for the $^{16}\text{O} + ^{164}\text{Dy}$ system in panels (a)–(e) and the $^{12}\text{C} + ^{181}\text{Ta}$ system in panels (f)–(j), respectively.

$\rho(E_X, J)$ used in the PACE2 calculations for an excitation energy above $E_X \sim 5$ MeV is given:

$$\rho(E_X, J) = \frac{(2J+1)}{12} \sqrt{a} \left(\frac{\hbar^2}{2\mathfrak{I}} \right)^{3/2} \frac{\exp(2\sqrt{aU})}{U_{\text{ex}}^2}, \quad (1)$$

where $U_{\text{ex}} = E_X - \Delta P(Z) - \Delta P(N)$ and $U = U_{\text{ex}} - E_{\text{rot}}$, where $E_{\text{rot}} = \frac{\hbar^2}{2\mathfrak{I}} J(J+1)$ is the rotational energy. $\Delta P(Z)$ and $\Delta P(N)$ are the ground-state pairing energy differences obtained from Gilbert and Cameron's compilation for odd-even mass differences. The moment of inertia \mathfrak{I} was calculated using Sierk rotating liquid drop model [14]. At E_X below ~ 5 MeV, Gilbert and Cameron's constant temperature formula was used for the level density. We used the following form for level-density parameter a [15], which is widely used in phenomenological descriptions of nuclear level density:

$$a = \tilde{a} \left\{ 1 - \frac{\Delta S}{U} [1 - \exp(-\gamma U)] \right\}, \quad (2)$$

where \tilde{a} is the asymptotic value of the level-density parameter and γ is the shell damping factor for which we have used the value 0.054 MeV^{-1} . The shell correction factor ΔS was calculated using the Swiatecki and Myers formalism [16], with the convention of being +ve for the closed shell nuclei. The value of \tilde{a} was externally varied in the code through the input card. The γ -ray decay intensities were taken from RIPL

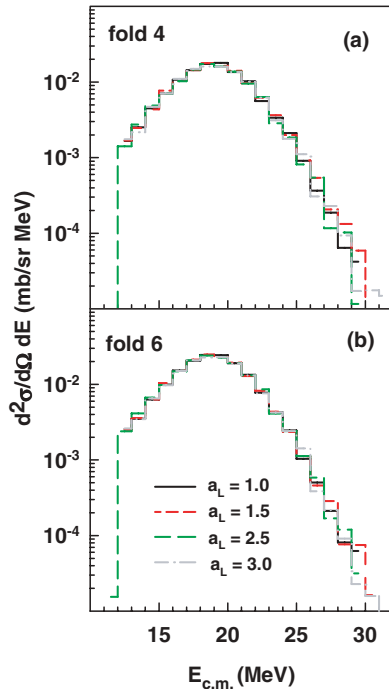


FIG. 2. (Color online) PACE2 calculated α -particle spectra for folds 4 and 6 for the $^{12}\text{C} + ^{181}\text{Ta}$ system in panels (a)–(b). Solid, short-dash, medium-dash, and dash-dot histograms are for the diffuseness parameter $a_L = 1.0, 1.5, 2.5,$ and 3.0 , respectively.

compilation [17]. The values of target and projectile spins were also provided in the input. The transmission coefficient as a function of energy and orbital angular momentum of the emitted particle is conventionally generated by the optical model potentials (OMPs). In these calculations for α -particle emission, the OMP parameters of Igo and Huizenga [18] were used. The initial angular momentum distribution for the compound nucleus was obtained from the Bass systematics [19] for fusion cross section with an angular momentum diffuseness parameter, $a_L = 0.5 \hbar$. We have examined the effect of compound nucleus spin distribution on the slope of the high-energy part of α -spectrum by varying diffuseness parameter a_L from 1.0 to 3.0. It is observed that the change in the slope of the PACE2-calculated fold-gated α -particle spectrum is $<1\%$ by changing a_L from 1.0 to 3.0, as shown in Fig. 2 for folds 4 and 6 in the $^{12}\text{C} + ^{181}\text{Ta}$ reaction for level-density parameter $\tilde{a} = A/8$.

Because of the limited efficiency of γ -ray detection and the uncertainty of angular momentum carried by individual γ -ray, it is not possible to convert γ -ray fold to spin value on an event-by-event basis. Each γ -ray fold corresponds to a window of the angular momentum populated in the residual nuclei. An average angular momentum, $\langle J \rangle$, corresponding to each γ -ray fold was assigned using the following procedure as discussed in detail in Ref. [11]. A multiplicity-versus-fold response 2D matrix for this BGO setup was generated. For each reaction, the residue spin distribution after α -particle emission (J_{res}) was determined using the trace-back feature of the PACE2 code. The residue spin distribution J_{res} was converted to γ -ray multiplicity strength distribution M , using the prescription $M = J_{\text{res}}/a_m$

as has been used in literature [7,20]. The parameter a_m was chosen to be 1.5. The multiplicity-versus-fold response 2D matrix was weighted according to γ -ray multiplicity strength distribution M for a specific residue spin distribution. Finally, by projecting this weighted BGO response 2D matrix on the fold axis, weighted multiplicity distribution was obtained for each fold. The mean of this distribution, $\langle M \rangle$, corresponding to a particular fold was again converted back to the first moment (average value of angular momentum) $\langle J \rangle$, using the relation $\langle J \rangle = \langle M \rangle a_m$. In similar fashion, the second moment of the distribution $\langle J^2 \rangle$ for each fold was calculated. From here, the width of the angular momentum window for each fold was deduced as follows:

$$\delta J = \sqrt{\langle J^2 \rangle - \langle J \rangle^2}. \quad (3)$$

The width δJ is large for lower folds and small for higher folds for each reaction. The uncertainty (width δJ) in the assignment of $\langle J \rangle$ varied from ± 5 to $\pm 3 \hbar$ in going from fold 4 to fold 11. Although 14 γ -detectors were used in the experiment, we got fold distribution up to fold value 11 only. The event distribution as a function of fold falls off exponentially. Thus, in a typical event distribution the counts in fold 11 are less than 1% of the total.

As mentioned previously, in this analysis the parameter a_m was chosen to be 1.5. We have examined the dependence of slope of the α -particle spectrum as a function of the parameter a_m for each fold. It is observed that the slope of the fold-gated spectrum does not change with parameter a_m as shown in Fig. 3, where PACE2 calculations are shown for the $^{12}\text{C} + ^{181}\text{Ta}$ system for various values of a_m . The level-density parameter \tilde{a} and diffuseness parameter a_L used in the calculations are $A/8$ and 1.0, respectively. The plots for $a_m = 1.5$ and 1.9 are scaled to $a_m = 1.0$, using the appropriate scaling factor SF. The value of SF for fold 4 is 0.64 for $a_m = 1.5$ and 0.62 for $a_m = 1.9$, whereas for fold 6 it is 1.4 for $a_m = 1.5$ and 2.5 for $a_m = 1.9$. Therefore, by varying parameter a_m , PACE2-calculated α -particle multiplicity changes but the slope of the spectrum remains unchanged. The structure effect of residual nuclei can affect the γ -ray multiplicity depending on the odd or even nature of residual nuclei. In this analysis we are getting an average γ -ray multiplicity and the spin value of residual nuclei. There may be some uncertainty on the absolute value of spin determination. But the results on the dependence of inverse level-density parameter on average spin of the residue will not be affected.

In this work, the inverse level-density parameter K is determined by comparing the shape of the fold-gated and summed α -particle spectra for fold 4 and above events with corresponding spectra obtained from PACE2 calculations. By limiting the analysis to the spectral shape at well above evaporation barrier, the uncertainties associated with the barrier transmission coefficients are avoided. The normalization of the shape of the experimental spectra with that obtained from the statistical model calculation was done by matching the area under the predicted spectra in the selected energy interval with that of the experimental spectra in the same energy interval. No attempts were made to fit the multiplicity of α -particles.

We have used the least-squares method to analyze the data to extract the most probable value and corresponding

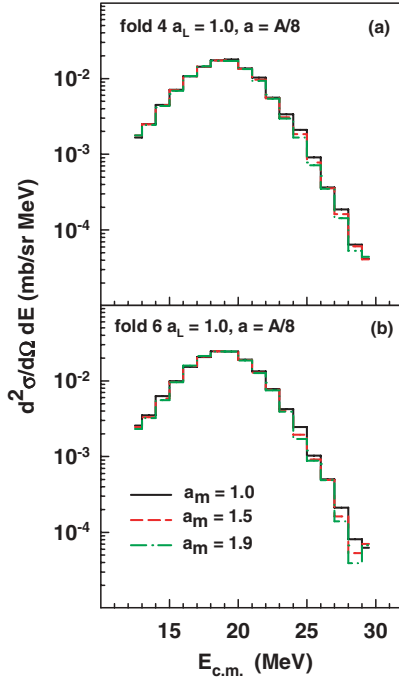


FIG. 3. (Color online) PACE2 calculated α -particle spectra for folds 4 and 6 for the $^{12}\text{C} + ^{181}\text{Ta}$ system in (a) and (b). Solid, short-dash, and dash-dot histograms are for parameter $a_m = 1.0, 1.5,$ and $1.9,$ respectively. The level-density parameter \tilde{a} and diffuseness parameter a_L used in the calculations are $A/8$ and $1.0,$ respectively. The plots for $a_m = 1.5$ and 1.9 are scaled to $a_m = 1.0,$ using the appropriate scaling factor SF (see text).

variance of the inverse level-density parameter K . The inverse level-density parameter was varied to fit the energy spectrum. The α -particle energy spectrum is a nonlinear function and the least-square solutions are determined by minimizing the statistical variance given:

$$S(K) = \sum_{i=1}^N \frac{[Y_i - f(K, E_i)]^2}{\sigma_i^2}, \quad (4)$$

where Y_i is the double differential cross section in the i th energy bin, $f(K, E_i)$ is the result of the PACE2 calculation for the same energy bin for the inverse level-density parameter K after normalization of the spectrum as discussed previously, and σ_i is the statistical error in the measured cross section. The energy region in α -particle spectra to calculate the $S(K)$ value was chosen from 21.5 to 31.5 MeV for all of the systems. We have evaluated $S(K)$ as a function of K using the above equation and, in most cases, a parabolic dependence of $S(K)$ on the parameter K was observed. Best-fit parameter \bar{K} was determined from the minimum of the parabola. The error δK on \bar{K} was determined with a 68.3% confidence level as discussed in Refs. [11,21].

IV. RESULTS AND DISCUSSION

The α -particle evaporation multiplicity ν_α for various γ -ray fold events was estimated from the measured evaporation

cross section and total fusion cross section. The α -particle multiplicity calculated using the PACE2 code was found to be of similar magnitude. According to the PACE2 calculations, a major fraction of the α particles ($\sim 92\%$) are emitted as first-chance emission for the center-of-mass α -particle energy interval 21.5–31.5 MeV. It is, therefore, assumed that the α -particle emission leaves residual nuclei with $Z = Z_{\text{CN}} - 2$ in this analysis, where Z_{CN} is the charge of the compound nucleus. However, residue mass has a broadening of one or two units, but there is no broadening in residue charge from non-selection of the exit channel. The residual nucleus excitation energy range corresponding to this set of measurements was estimated as follows. The excitation energy after first-chance α -particle emission is given by

$$E_X = E_{\text{ex}}^{\text{CN}} - S_\alpha - E_\alpha^{\text{c.m.}}, \quad (5)$$

where $E_{\text{ex}}^{\text{CN}}, S_\alpha,$ and $E_\alpha^{\text{c.m.}}$ are the initial excitation energy of the compound nucleus, α -particle separation energy, and kinetic energy of the emitted α particle, respectively. The $E_{\text{ex}}^{\text{CN}}$ and $E_\alpha^{\text{c.m.}}$ range were chosen such that the approximate range of E_X is between 30 and 40 MeV. The intrinsic excitation energy available for the residual nuclei, however, will be somewhat less than E_X by the energy locked in rotational energy of the nuclei, E_{rot} , which is around 2.2–2.6 MeV for this mass region for $J = 20 \hbar$.

Using the least-squares fit method, the experimental fold-gated spectra were compared with the corresponding PACE2 predictions. As mentioned earlier, the calculated α -particle yields at the selected high-energy region were normalized to the experimental yields while fitting the spectra. The measured fold-gated α -particle energy spectra for various γ -ray folds (open circles) and corresponding PACE2 best fits after the normalization (solid histograms), for all the systems, are shown in Figs. 4–7. The fold number, the K value obtained (with error bar), and experimental as well as calculated (in parentheses) α -particle multiplicity, ν_α , are shown at the bottom of each panel. The insets in the panels show the nearly parabolic variation of $S(K)$ with the parameter K . The minimum of the parabola corresponds to the best-fit value of the inverse level-density parameter K . The best-fit inverse level-density parameter K as a function of average angular momentum (corresponding to the γ -ray fold) $\langle J \rangle$ is shown in Fig. 8. The dotted lines in Fig. 8 are drawn as a guide to the eye to show the average behavior. It can be seen in Fig. 8 that within statistical errors the value of K is constant for each system over the angular momentum range of 15–30 \hbar . However, as mentioned earlier the uncertainty δJ in the value of $\langle J \rangle$ varies from ± 5 to $\pm 3 \hbar$ in going from fold 4 to fold 11, but the constant behavior of the parameter K as a function of angular momentum in this mass region remains unchanged. Similar observation was reported earlier by Henss *et al.* [22] for the $^{64}\text{Ni} + ^{92}\text{Zr}$ system, where the neutron evaporation spectra were measured by selecting only high-spin states of average spin $52 \hbar$ in the $^{155}\text{Er}^*$ nucleus. They obtained a value of level-density parameter $a = A/(8.8 \pm 1.3) \text{ MeV}^{-1}$ for $52 \hbar$ and for excitation energies between 30 and 36 MeV, which is close to the value of a for low spins and low excitation energy in nuclei of similar mass. In our earlier work [11], at around $Z = 50$ shell closure we obtained strong dependence of inverse

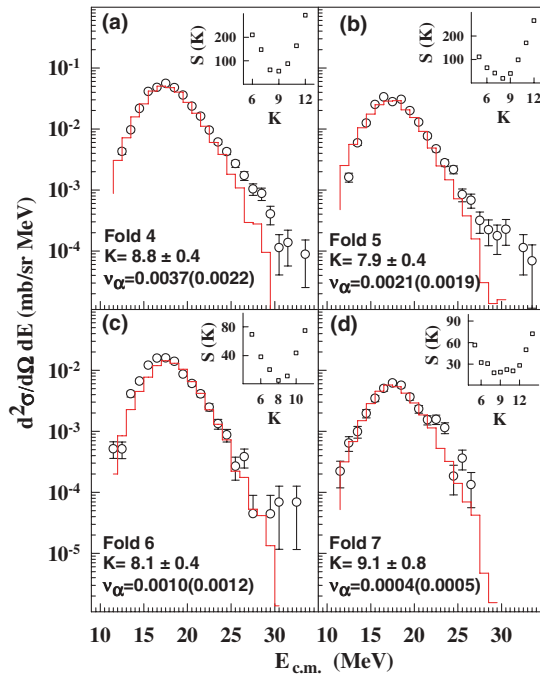


FIG. 4. (Color online) Fold-gated α -particle energy spectra in the center-of-mass system in the $^{11}\text{B} + ^{164}\text{Dy}$ reaction for various folds (open circles) in (a)–(d) along with the results of the PACE2 statistical model calculation (solid histograms). The fold number, the K value obtained (with error bar), and the experimental as well as the calculated (in parentheses) multiplicity of α -particles, ν_α , are shown at the bottom of each panel. In the inset, statistical variance is shown (open squares) as a function of K from where the best-fit K value was determined as discussed in the text.

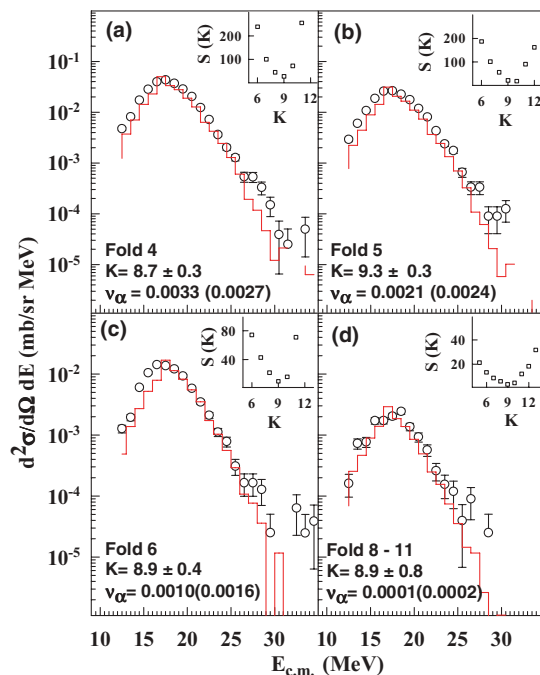


FIG. 5. (Color online) Same as Fig. 4 but for the $^{12}\text{C} + ^{164}\text{Dy}$ reaction.

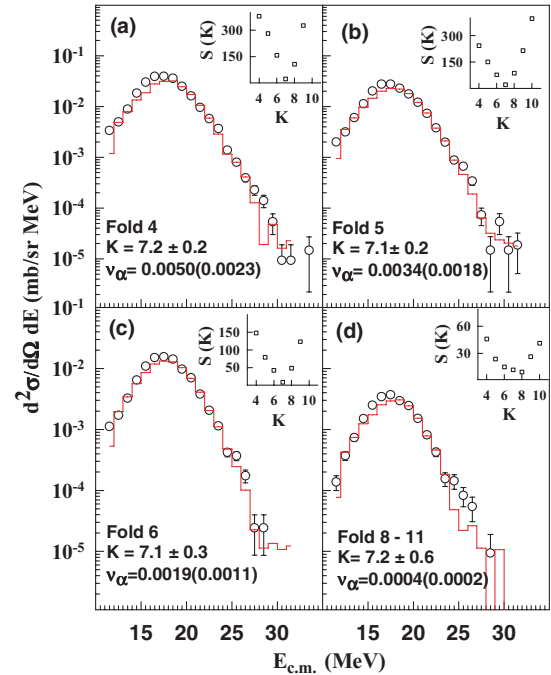


FIG. 6. (Color online) Same as Fig. 4 but for the $^{16}\text{O} + ^{164}\text{Dy}$ reaction.

level-density parameter K on angular momentum in the range of 15–30 \hbar in the $^{11}\text{B} + ^{115}\text{In}$ system ($Z_R = 52$) where the K value varied from 8.9 ± 0.4 MeV for low angular momentum to 15.3 ± 0.9 MeV for high angular momentum. However, in the midshell region studied in this work, the value of K remains nearly constant over an angular momentum range of 15–30 \hbar . There is no microscopic understanding of these observations,

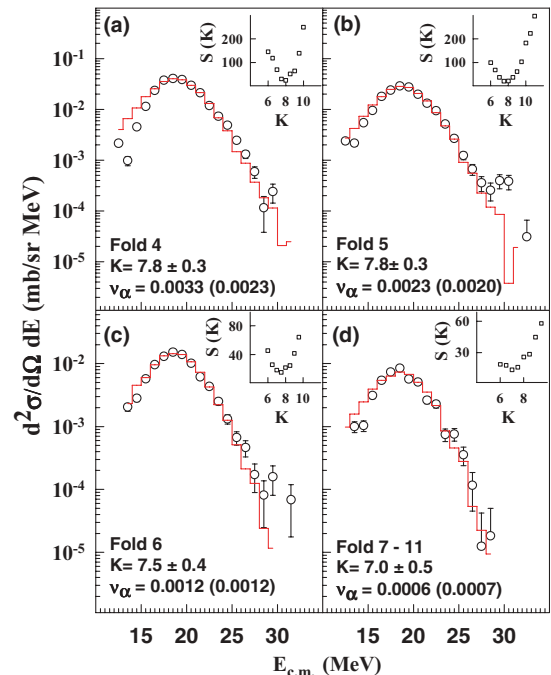


FIG. 7. (Color online) Same as Fig. 4 but for the $^{12}\text{C} + ^{181}\text{Ta}$ reaction.

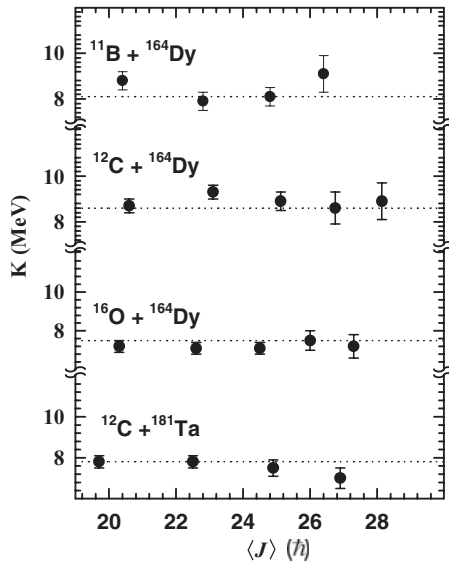


FIG. 8. Inverse level-density parameter K as a function of $\langle J \rangle$ (see text) for different systems. Dotted lines are shown to guide the eye.

but these experimental results will serve as important inputs for carrying out these calculations.

The gross energy spectra of α particles summed over all γ -ray folds of 4 and above were also compared with corresponding PACE2 predictions. The gross value of K for the summed spectrum was obtained using again the least-square fit method for each system. This gross value of K is plotted as a function of the charge of residual nuclei as shown in Fig. 9 (solid squares). The gross K values for nuclei studied in this work are around 8.2 ± 1.1 , as shown by the shaded region in Fig. 9. This value is consistent with systematics established for low excitation energy and spin [3]. In Fig. 9, we also show (open circles) the gross values of K (summed over all γ -ray fold events) for mass region ~ 120 ($Z_R = 48-55$) from Ref. [11]. It is seen that the gross value of K for the mass region 180 is lower than that for mass region 120. However, it may be noted that in mass region ~ 120 the gross

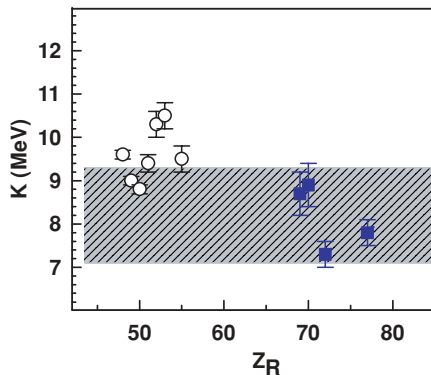


FIG. 9. (Color online) Inverse level-density parameter K determined from the summed spectra (see text) as a function of Z of residual nuclei. Open circles are from Ref. [11] and solid squares are from this work.

value of K determined from summed spectra for all γ -ray folds of 4 and above events is expected to be higher than the value corresponding to that summed over all γ -ray fold events because of the increase of K as a function of angular momentum in the range of $15-30 \hbar$. This will lead to further differences in gross K values for mass regions 120 and 180 than those shown in Fig. 9.

The entrance-channel mass-asymmetry parameter α in this experiment for mass region 180 is larger than that used for mass region 120. It has been pointed out earlier [23,24] that the high-energy slope of light-charged particle spectrum is affected by entrance-channel mass asymmetry. The effect of entrance-channel mass asymmetry in compound nucleus formation has been studied earlier in terms of mass-asymmetry parameter α with respect to α_{BG} (Businaro-Gallone critical mass asymmetry) [25]. Figure 10 shows the variation of α_{BG} as a function of angular momentum for all the systems studied in this work. It is seen that for all the systems studied, the value of mass-asymmetry parameter α is higher than α_{BG} for all J . Therefore, the entrance-channel effect with respect to the BG point is not expected to play a role for these systems. Similar conclusions were also drawn for mass region ~ 120 in our earlier work [11]. The lower value of K for mass region 180 than mass region 120 cannot be from the entrance-channel effect. It can be seen that the value of K is higher at $Z = 48-55$ (shell closure region) than at $Z \sim 70-77$ (midshell region). These results for the value of K seen over

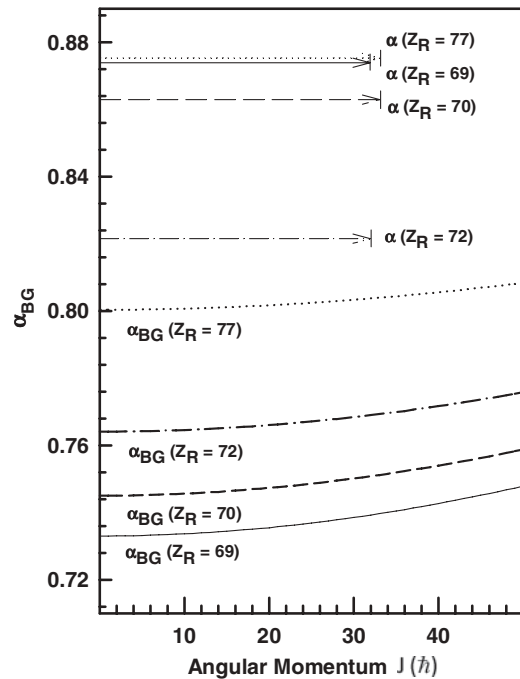


FIG. 10. The α_{BG} as a function of entrance-channel angular momentum J for all the reactions studied in this work. In the figure, the arrows on the Y axis indicate the position of mass-asymmetry parameter α for different target-projectile systems that terminate at the corresponding l_{gr} (see Table I). Corresponding to each reaction, the value of Z_R is shown along each line and arrow.

the entire range of $Z = 48\text{--}77$ imply the role of shell closure in the enhancement of K in the $Z = 50$ region.

V. SUMMARY

In this work, we have measured the γ -ray fold-gated α -particle energy spectra in reactions that populate residual nuclei in the regions of $Z \sim 70$ and $A \sim 180$ with an excitation energy in the range of 30–40 MeV. The high-energy part of the fold-gated and summed α -particle spectra for fold 4 and above were least-square fitted with the statistical model PACE2 predictions to determine the inverse level-density parameter $K = A/a$. The average value of K in this mass region is 8.2 ± 1.1 , and does not show any significant dependence on angular momentum in the range of 15–30 \hbar . These results for nuclei in

the midshell region ($Z \sim 70$), along with the results presented in one of our earlier works [11] in the shell closure region ($Z \sim 50$), could serve as important inputs for microscopic theories to understand the statistical properties of nuclei in different mass regions.

ACKNOWLEDGMENTS

We are thankful to the operating staff of the Pelletron accelerator for making available the required beams, and to D. R. Chakrabarty, Suresh Kumar, R. G. Thomas, R. P. Vind, A. L. Inkar, and R. V. Jangale for their help during the experiments. We also thank A. Mitra, A. Chatterjee, S. S. Kapoor, and S. Kailas for fruitful discussions and encouragement.

-
- [1] W. Dilg, W. Schantl, H. Vonach, and M. Uhl, Nucl. Phys. **A217**, 269 (1973).
- [2] R. Stokstad, in *Treatise on Heavy Ion Science*, edited by D. A. Bromley (Plenum, New York, 1985), Vol. 3, p. 83.
- [3] A. S. Ijtinov, M. V. Mebel, N. Bianchi, E. D. Sanctis, C. Guaraldo, V. Lucherini, V. Muccifora, E. Polli, A. R. Reolon, and P. Rossi, Nucl. Phys. **A543**, 517 (1992).
- [4] M. Beckerman, Nucl. Phys. **A278**, 333 (1977).
- [5] D. R. Chakrabarty, V. M. Datar, S. Kumar, E. T. Mirgule, H. H. Oza, and U. K. Pal, Phys. Rev. C **51**, 2942 (1995).
- [6] B. John, R. K. Choudhury, B. K. Nayak, A. Saxena, and D. C. Biswas, Phys. Rev. C **63**, 054301 (2001).
- [7] A. Mitra, D. R. Chakrabarty, V. M. Datar, S. Kumar, E. T. Mirgule, H. H. Oza, V. Nanal, and R. G. Pillay, Nucl. Phys. **A765**, 277 (2006).
- [8] N. G. Nicolis, D. G. Sarantites, L. A. Adler, F. A. Dilmanian, K. Honkanen, Z. Majka, L. G. Sobotka, Z. Li, T. M. Semkow, J. R. Beene *et al.*, Phys. Rev. C **41**, 2118 (1990).
- [9] M. Lunardon, C. Merigliano, G. Viesti, D. Fabris, G. Nebbia, M. Cinausero, G. de Angelis, E. Farnea, E. Fioretto, G. Prete *et al.*, Nucl. Phys. **A652**, 3 (1999).
- [10] G. Viesti, M. Lunardon, D. Bazzacco, R. Burch, D. Fabris, S. Lunardi, N. H. Medina, G. Nebbia, C. R. Alvarez, G. de Angelis *et al.*, Phys. Lett. **B382**, 24 (1996).
- [11] Y. K. Gupta, B. John, D. C. Biswas, B. K. Nayak, A. Saxena, and R. K. Choudhury, Phys. Rev. C **78**, 054609 (2008).
- [12] A. Gavron, Phys. Rev. C **21**, 230 (1980).
- [13] H. Ho and P. L. Gonthier, Nucl. Instrum. Methods **190**, 75 (1981).
- [14] A. J. Sierk, Phys. Rev. C **33**, 2039 (1986).
- [15] A. V. Ignatyuk, G. N. Smirenkin, and A. S. Tishin, Sov. J. Phys. **21**, 255 (1975).
- [16] P. Moller, J. R. Nix, W. D. Myers, and W. J. Swiatecki, At. Data Nucl. Data Tables **59**, 185 (1995).
- [17] International Atomic Energy Agency, *Handbook for Calculations of Nuclear Reaction Data: Reference Input Parameter Library, RIPL-2*, Vienna, 2005, <http://www-nds.iaea.org/RIPL-2>, IAEA-Tecdoc-1506.
- [18] J. R. Huizenga and G. Igo, Nucl. Phys. **29**, 462 (1962).
- [19] R. Bass, Phys. Rev. Lett. **39**, 265 (1977).
- [20] B. K. Nayak, R. K. Choudhury, L. M. Pant, D. M. Nadkarni, and S. S. Kapoor, Phys. Rev. C **52**, 3081 (1995).
- [21] D. Cline and P. M. S. Lesser, Nucl. Instrum. Methods **82**, 291 (1970).
- [22] S. Henss, A. Ruckelshausen, R. D. Fischer, W. Kuhn, V. Metag, R. Novotny, R. V. F. Janssens, T. L. Khoo, D. Habs, D. Schwalm *et al.*, Phys. Rev. Lett. **60**, 11 (1988).
- [23] J. F. Liang, J. D. Bierman, M. P. Kelly, A. A. Sonzogni, R. Vandenbosch, and J. P. S. van Schagen, Phys. Rev. Lett. **78**, 3074 (1997).
- [24] I. M. Govil, R. Singh, A. Kumar, J. Kaur, A. K. Sinha, N. Madhavan, D. O. Kataria, P. Sugathan, S. K. Kataria, K. Kumar *et al.*, Phys. Rev. C **57**, 1269 (1998).
- [25] M. Abe, KEK Report No. 86-26, KEK TH-128, 1986.